Supporting information

Constructing $ZnIn_2S_4$ nanoparticles/MoS_2-RGO nanosheets 0D/2D heterojunction for significantly enhanced visible-light photocatalytic H_2 production

Zhongjie Guan [a,b,*], Peng Wang [a], Qiuye Li [a,*], Guoqiang Li[b], Jianjun Yang [a]

[a]National & Local Joint Engineering Research Center for Applied Technology of Hybrid Nanomaterials, Collaborative Innovation Center of Nano Functional Materials and Applications of Henan Province, Henan University, Kaifeng 475004, China

[b]Key Laboratory of Photovoltaic Materials of Henan Province, School of Physics & Electronics, Henan University, Kaifeng 475004, China

*To whom correspondence should be addressed, E-mail: guanzj@henu.edu.cn; qiuyeli@henu.edu.cn

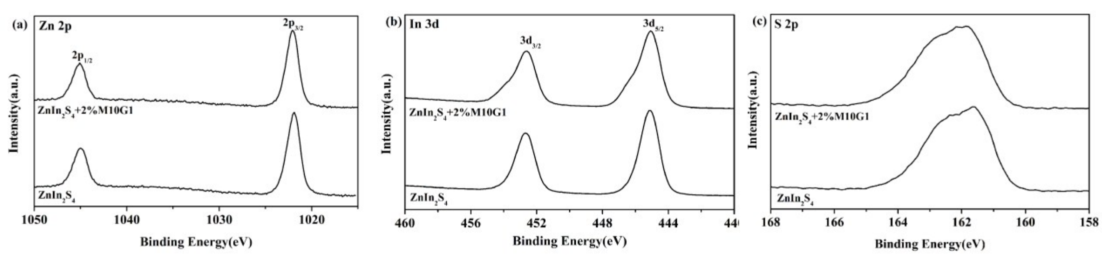

Fig. S1 XPS spectra of Zn 2p (a), In 3d (b) and S 2p (c) for pure $ZnIn_2S_4$ and $ZnIn_2S_4$+2%M10G1 composite samples.

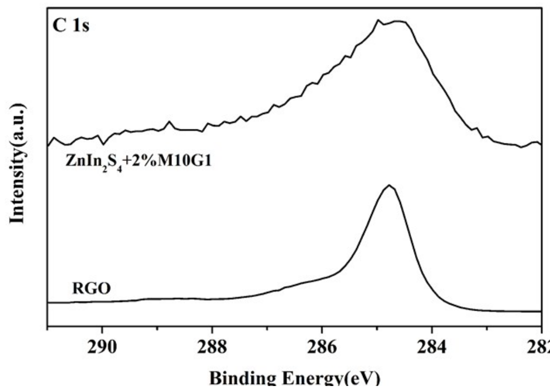

Fig. S2 XPS spectra of C 1s for RGO and $ZnIn_2S_4$+2%M10G1 composite sample.

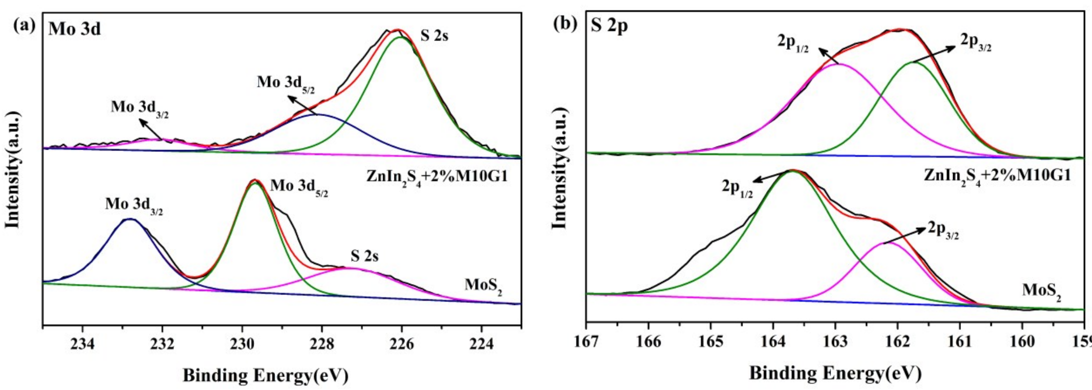

Fig. S3 XPS spectra of Mo 3d (a) and S 2p (b) for MoS_2 and $ZnIn_2S_4$+2%M10G1 composite samples.

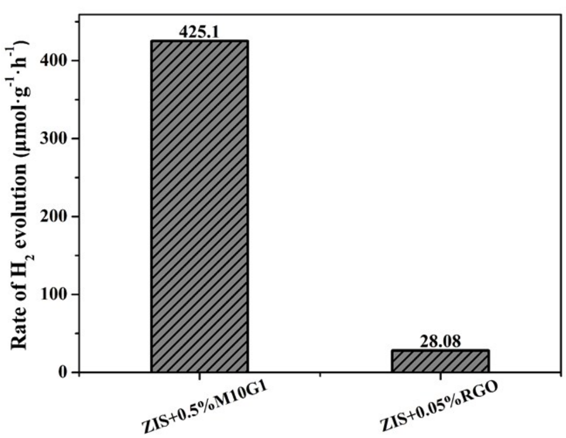

Fig. S4 H_2 evolution rates of $ZnIn_2S_4$+0.5%M10G1 and $ZnIn_2S_4$+0.05%RGO samples under visible light irradiation (λ>420 nm).

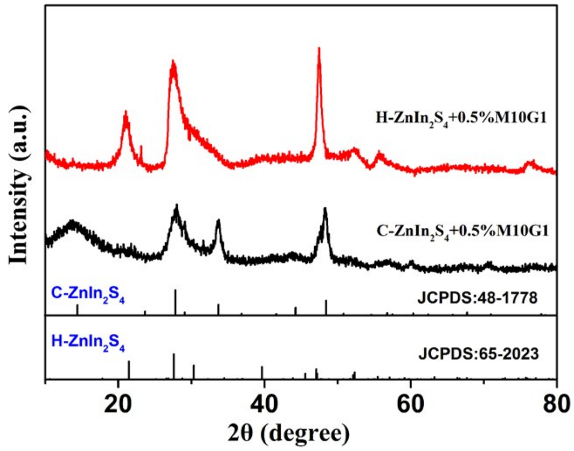

Fig. S5 XRD patterns of cubic $ZnIn_2S_4$+0.5%M10G1 and hexagonal $ZnIn_2S_4$+0.5%M10G1 samples.

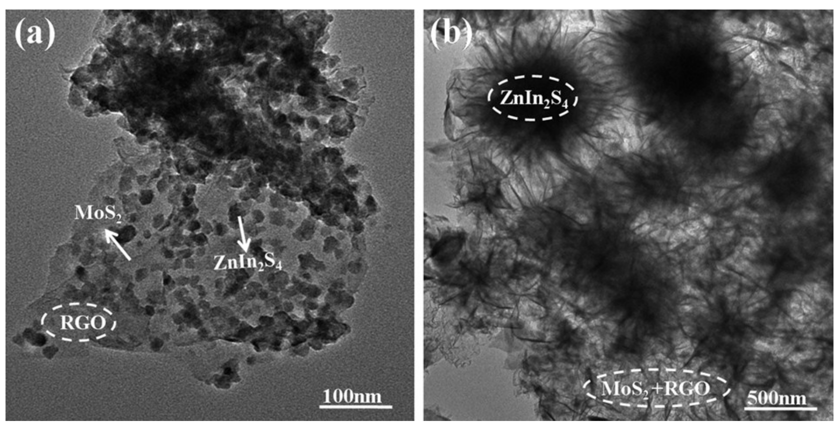

Fig. S6 TEM images of cubic $ZnIn_2S_4$+0.5%M10G1 (a) and hexagonal $ZnIn_2S_4$+0.5%M10G1samples (b).

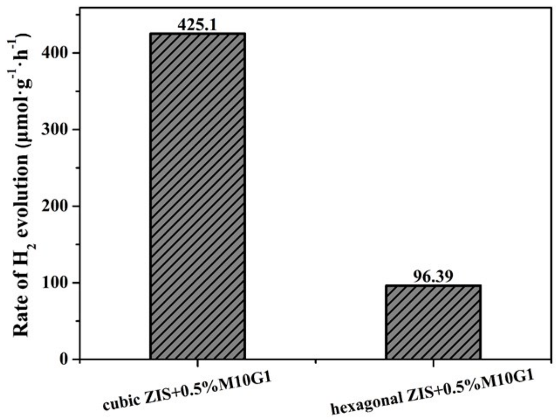

Fig. S7 H_2 evolution rates of cubic $ZnIn_2S_4$+0.5%M10G1 and hexagonal $ZnIn_2S_4$+0.5%M10G1 samples under visible light irradiation (λ>420 nm).

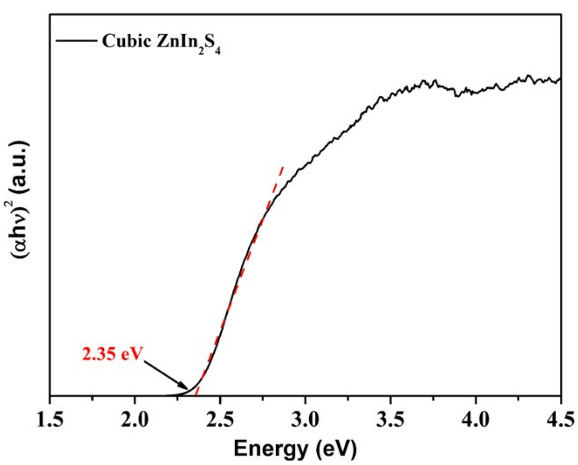

Fig. S8 The plots of $(\alpha h\nu)^2$ vs. hν for cubic $ZnIn_2S_4$.